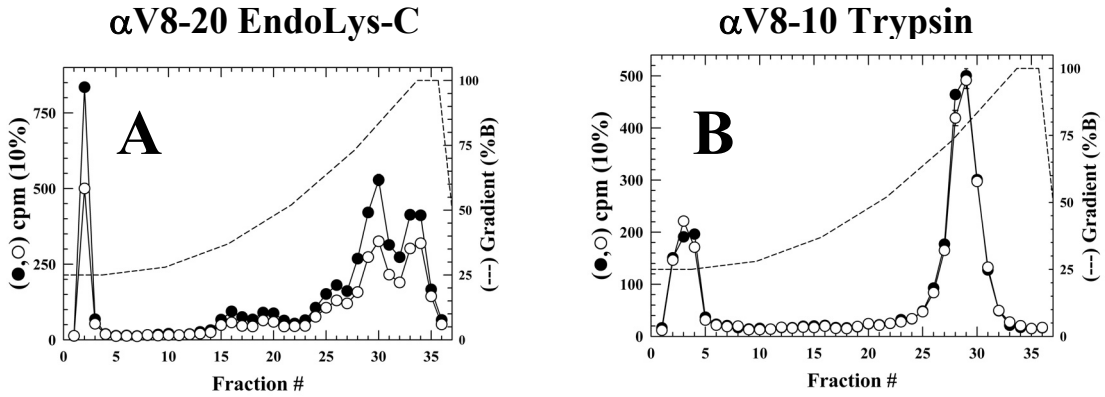


**Supplemental Figure S1. Isolation of [$^3$H]TDBzl-Etomidate-labeled αM2 and αM4 by reversed-phase HPLC fractionation of EndoLys-C digests of αV8-20 (A) and trypsin digests of αV8-10 (B).** The α subunits were isolated from nAChR-rich membranes photolabeled with 1 μM [$^3$H]TDBzl-Etomidate in the absence (●) or presence (○) of 0.1 mM tetracaine. V8 protease digests of the α subunits were fractionated by SDS-PAGE (Experimental Procedures), visualized by Coomassie blue stain, and material was eluted from the gel bands containing αV8-20 and αV8-10. Digests were fractionated by reversed-phase HPLC. 10 % of each fraction was assayed for $^3$H (●, ○), and also plotted as dashed lines are the HPLC gradients in percent solvent B (organic phase). **A**, Fractionation of EndoLys-C digests of the αV8-20 samples (–tetracaine, 56,000 cpm injected, 85 % recovered; +tetracaine, 27,000 injected, 118 % recovered). Sequence analysis of the pools of fractions 33 & 34 (20% of recovered $^3$H), which contained a fragment beginning at the N-terminus of αM2 (αMet-249), are shown in Figure 5A. **B**, Fractionation of trypsin digests of αV8-10 (–tetracaine, 26,000 cpm injected, 91 % recovered; +tetracaine, 24,000 injected, 95 % recovered). Sequence analysis of the pools of fractions 28-30 (80 % organic, ~51 % of recovered $^3$H) identified αTyr-401 (1.5 pmol in each sample), consistent with the sequencing data in Figure 8 from a different preparative labeling.

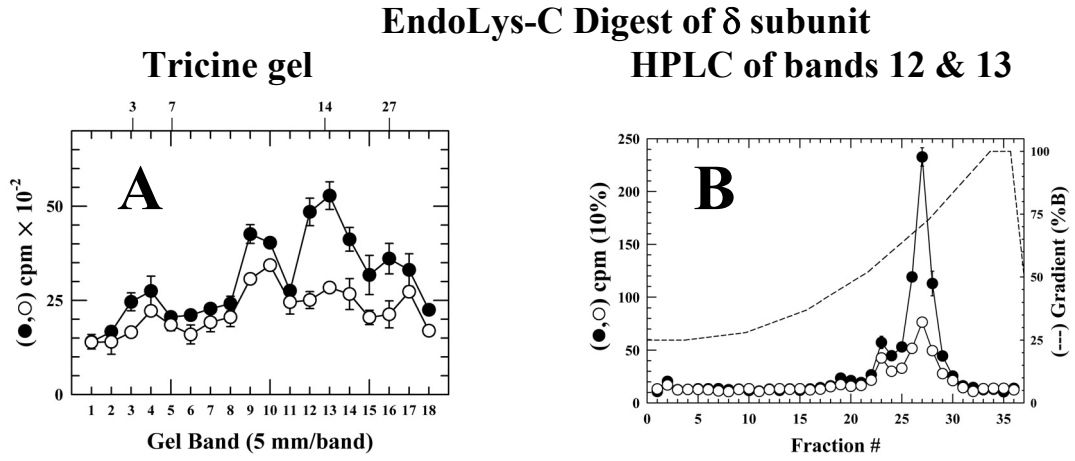


**Supplemental Figure S2: Fractionation of EndoLys-C digests of [$^3$H]TDBzl-Etomidate-labeled δ subunit by Tricine-SDS PAGE (A) and purification by reversed-phase HPLC of the fragments beginning at δMet-257 (δM2) and δPhe-206 (δM1)..** δ subunits isolated from the same labeling described in Supplemental Figure S1 were digested with EndoLys-C, and the digests were fractionated by Tricine SDS-PAGE. **A,** The distribution of $^3$H eluted from 5 mm bands of each lane of the gel (1% counted, ●, –tetracaine, 52,500 cpm digested, 32,000 cpm recovered; ○, +tetracaine, 36,700 cpm digested, 21,600 cpm recovered). The mobilities of the molecular mass markers are denoted above the graph. **B,** Reversed-phase HPLC fractionation of the material eluted from gel bands 12 and 13 (~12-14 kDa) (●, –tetracaine, 7,730 cpm injected, 87 % recovered; ○, +tetracaine, 3,100 injected, 91 % recovered). The HPLC gradient in percent solvent B (organic phase) is plotted as a dashed line (---). Sequence analysis of the pools of fractions 26-28 (70% organic, ~60 % of recovered $^3$H), which contained a fragment beginning at the N-terminus of δM2, are shown in Figure 5C. Sequence analysis of the pools of fractions 22 and 23 identified a fragment beginning at δPhe-206 (7 pmol) that extended through δM1.

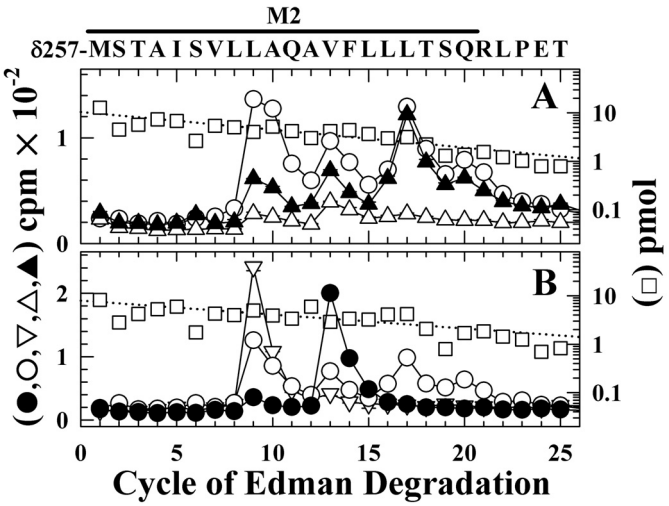


**Supplemental Figure S3. [$^3$H]TDBzl-Etomidate labeling within the δM2 in the presence of PCP or proadifen.** $^3$H (○, ▲, △, ▽, ●) and PTH-amino acids (□) released during sequencing of δ subunit fragments beginning at the N-terminus of δM2. The primary amino acid sequence is shown above the top panel. **A,** From the photolabeling experiment of Figures 6A and B, the fragments beginning at δMet-257 were purified by Tricine-gel SDS-PAGE and reversed phase HPLC from EndoLys-C digests of δ subunits from nAChRs photolabeled +Carb (○,□, $I_0$ = 10 pmol), +Carb+PCP (▲, $I_0$ = 20 pmol), and +PCP (△, $I_0$ = 12 pmol). For nAChRs labeled +Carb, the $^3$H releases in cycles 9, 13, 16, 17 and 20 indicated labeling (in cpm/pmol) of δLeu-265 (5), δVal-269 (3), δLeu-272 (2), δLeu-273 (6), and δGln-276 (2), which for the sample +Carb +PCP was reduced by 80% and 70% at δLeu-265 (0.8 cpm/pmol), and δVal-269 (0.9 cpm/pmol), and by ~50% at δLeu-273 (3.1 cpm/pmol) and δGln-276 (1 cpm/pmol). For nAChRs labeled +PCP, δLeu-265 (0.6 cpm/pmol) and δVal-269 (1.3 cpm/pmol) were labeled at similar efficiencies as for those labeled +Carb+PCP. **B**, From the photolabeling of Fig. 5 D, the fragments beginning at δMet-257 were isolated from the nAChRs photolabeled in the absence of any ligand (●), + proadifen (▽) or +Carb (○). The $I_0$ for the primary sequences of each sample was between 8 – 9 pmol. For nAChRs labeled in the absence of other drugs, the primary release of $^3$H was at cycle 13, corresponding to labeling of δVal-269 at 13 cpm/pmol, and that labeling was reduced by > 95% in the presence of proadifen. In contrast, in the presence of proadifen, the major peak of $^3$H release was in cycle 9, corresponding to labeling of δLeu265 (10 cpm/pmol) at ~10-fold higher efficiency than in the control (1 cpm/pmol). The preferential photolabeling of δM2-9 +proadifen was distinct from that seen +Carb (○), with labeling of δM2 -9, -13, -16, -17, and -20.

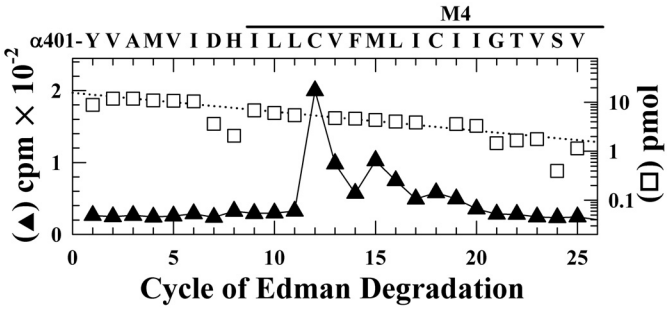


**Supplemental Figure S4. [$^3$H]TDBzl-Etomidate photolabeling within αM4.** $^3$H (▲) and PTH-amino acids (□) released during sequencing of fragments isolated from trypsin digests of αV8-10, isolated by reversed phase HPLC from nAChRs photolabeled +Carb +PCP as described in Figure 6A. The only sequence detected began at αTyr-401 ($I_0$ = 15 pmol), and the peaks of $^3$H release in cycles 12 and 13 indicate labeling within αM4 of αCys-412 and αMet-415 at 7 and 5 cpm/pmol.

**Supplemental Figure S5. Stereo representations of the TDBzl-Etomidate binding pocket at the γ-α interface in the nAChR transmembrane domain** (see next page for Figure Legend).

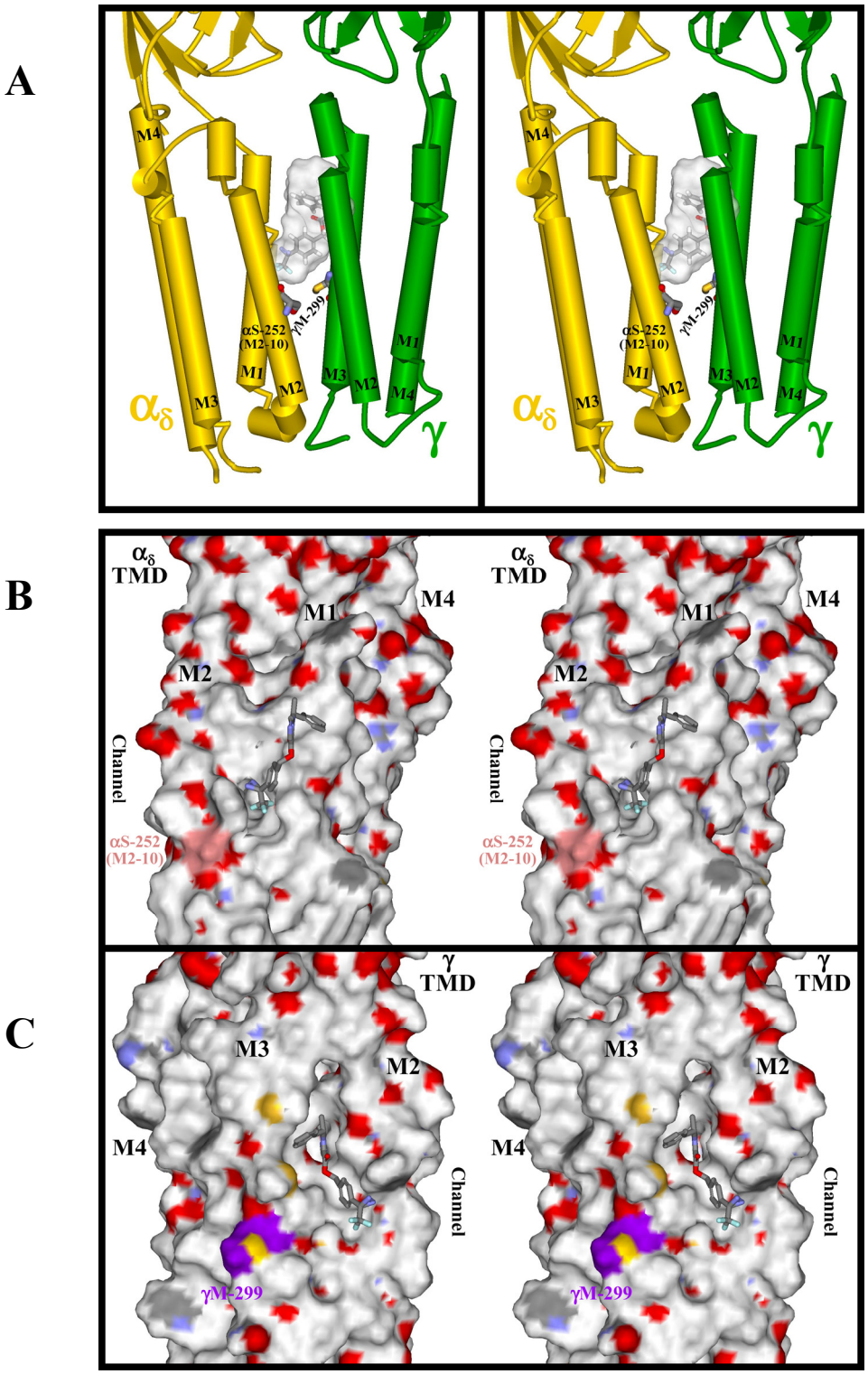

**Supplemental Figure S5: Stereo representations of TDBzl-Etomidate binding pocket at the γ-α interface in the nAChR transmembrane domain.** Expanded views are presented of portions of the *T. californica* nAChR homology model (Figure 8, α (gold), γ (green)).

**A**, A view of the transmembrane helical bundles (shown as cylinders) of the α and γ subunits with the volumes defined by 10 docked TDBzl-Etomidates in the pocket between the γ and α subunits shown as a Connolly surface representation (white). Also included in stick format are the photolabeled residues and a TDBzl-Etomidate molecule docked in its lowest energy orientation (Experimental Procedures).

**B & C**, Stereo images of the α (**B**) and γ (**C**) transmembrane helical bundles, viewed as Connolly surface representations from the γ-α interface. The images illustrate each subunit's contribution to the TDBzl-Etomidate binding pocket, which is identified by a TDBzl-Etomidate docked in its lowest energy orientation. The surface exposures of αSer-252 (pink, in **B**) and γMet-299 (purple, in **C**) are also shown. Otherwise, color-coding represents atom type: H, white; C, gray; O, red; N, blue; and S, yellow. For orientation, the visible helices are denoted, as is the relative location of the ion channel in each figure.

**Supplemental Figure S6. Stereo representations of TDBzl-Etomidate binding sites in the nAChR transmembrane domain.** Expanded views are presented of portions of the *T. californica* nAChR homology model (Figure 8, α (gold), β (blue), γ (green); δ (magenta)).

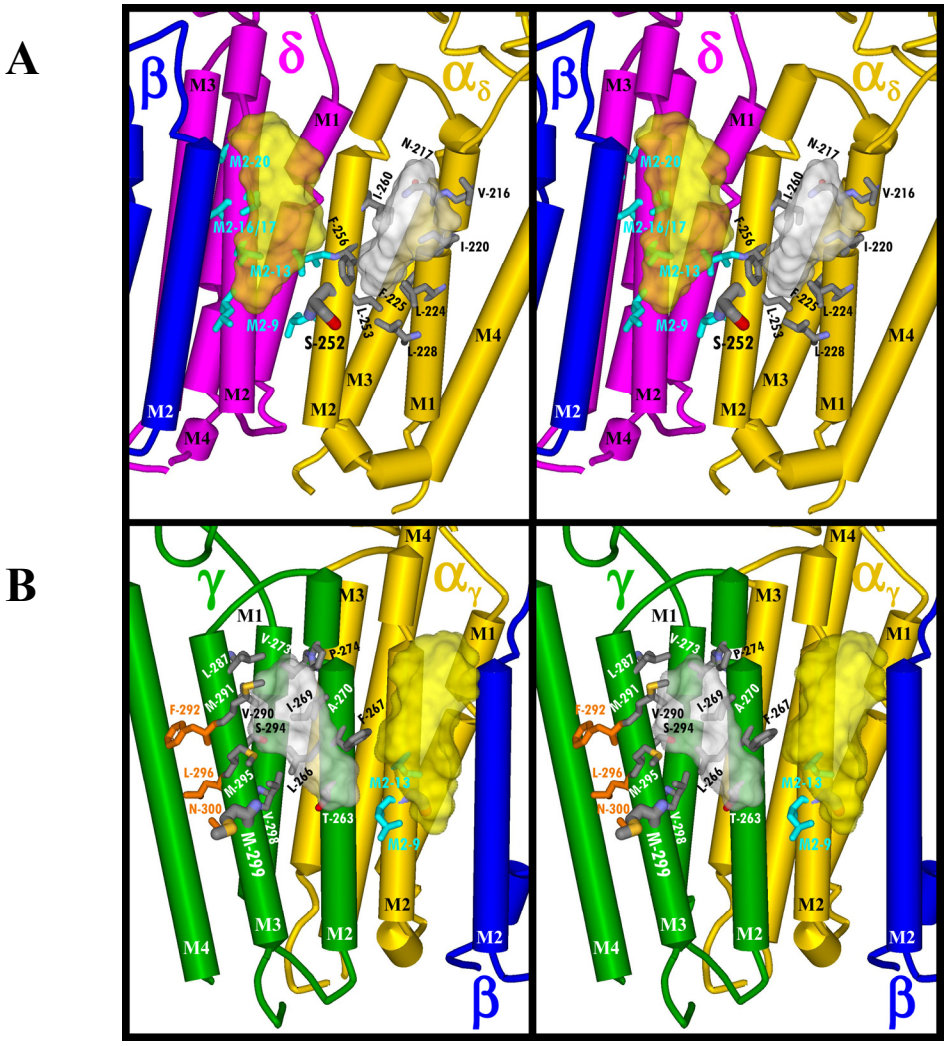


**A**, A view from the γ subunit towards the $\alpha_\delta$ subunit TMD, with the amino acids of αM1 and αM2 shown in stick format that can contribute to the binding pocket at the γ-α interface (shown in white). **B**, A view from the $\alpha_\delta$ subunit towards the γ subunit TMD, with the amino acids of γM2 and γM3 shown in stick format that can contribute to the binding pocket at the γ-$\alpha_\delta$ interface (shown in white). Also shown in cyan are the residues of the α and δ subunits in the lumen of the ion channel that were labeled by TDBzl-Etomidate. The volumes of the ensemble of 10 TDBzl-Etomidates docked within the channel lumen (yellow, volume 900 $Å^3$) or the γ-α interface (white, volume 580 $Å^3$) are shown in Connolly surface representations. Residues labeled by [$^{125}$I]TID from the protein-lipid interface (γPhe-292, γLeu-296, and γAsn-300) are shown in orange (Blanton and Cohen, Biochemistry 33: 2859 (1994)). Within γM3, γMet-291 and γMet-295, which were not labeled by [$^3$H]TDBzl-Etomidate, project towards the interface pocket. Those residues were also not labeled by [$^{125}$I]TID from the protein-lipid interface.